IJRCS

International Journal of Robotics and Control Systems
Vol. 5, No. 3, 2025, pp. 1975-1997
ISSN 2775-2658
http://pubs2.ascee.org/index.php/ijrcs

ASCEE

Optimization of a Robust Sigmoid PID Controller for Automatic Voltage Regulation Using the Nonlinear Sine-Cosine Algorithm with Amplifier Feedback Dynamic Weighted (AFDW) System

Islam Ahmed [a,1,*], Mohd Helmi Suid [a,2], Mohd Ashraf Ahmad [a,3], Salmiah Ahmad [b,4], Mohd Falfazli Mat Jusof [a,5], Zaidi Mohd Tumari [c,6]

[a] Faculty of Electrical and Electronics Engineering Technology, Universiti Malaysia Pahang Al-Sultan Abdullah, Pahang, Malaysia
[b] College of Engineering and Technology, University of Doha for Science and Technology, Doha, 24449, Qatar
[c] Faculty of Electrical and Electronics Engineering Technology Universiti Teknikal Malaysia Melaka, Melaka, Malaysia
[1] islamkhan45374@gmail.com; [2] mhelmi@umpsa.edu.my; [3] mashraf@umpsa.edu.my; [4] salmiah.ahmad@udst.edu.qa; [5] mfalfazli@umpsa.edu.my; [6] mohdzaidi.tumari@utem.edu.my
* Corresponding Author

ARTICLE INFO

Article history
Received May 16, 2025
Revised July 24, 2025
Accepted October 04, 2025

Keywords
Automatic Voltage Regulator;
Sigmoid PID Controller;
Metaheuristic Optimization;
Nonlinear Sine-Cosine Algorithm

ABSTRACT

The given paper presents a robust Sigmoid-based Proportional-Integral-Derivative (SPID) controller for Automatic Voltage Regulator (AVR) systems, optimized using the Nonlinear Sine Cosine Algorithm (NSCA) enhanced with the Amplifier Feedback Dynamic Weighted (AFDW) system. Conventional PID controllers are frequently struggling with parameter variations and external interruptions that lead to instability and reduced performances in AVR systems. The proposed SPID controller overcomes these limitations by incorporating nonlinear sigmoid functions, improving the AVR system's robustness and dynamic response. While the AFDW system improves stability and responsiveness by dynamically adjusting the feedback weight, the NSCA balances exploration and exploitation to optimize controller parameters. The primary contribution of the present research is an overview of the NSCA-SPID controller, which offers superior results in voltage regulation compared to traditional PID and other metaheuristic-tuned controllers, enhancement in settling time, elimination of overshoot, and improvement in steady-state error. Additionally, performance index and statistical performances are used to validate the proposed SPID controller. Simulation results demonstrate significant achievements that emphasize the effectiveness of the NSCA-SPID controller toward enhancing the AVR system stability and controller design's performance under varying load conditions. Finally, the proposed NSCA-SPID controller provides a promising solution for Enhancing the regulation of voltage in power systems, providing Superior and efficient technique for practical applications.

1. Introduction

An automatic voltage regulator (AVR) is a crucial part of current electrical power systems since it keeps the voltage steady, particularly in synchronous generator systems. These regulators maintain a constant voltage level despite fluctuating in load conditions, therefore maintaining grid stability and improving efficiency during operation. In industrial applications, AVRs serve as crucial for protecting sensitive appliances, producing the consistent voltage required for electrical equipment to operate effectively and safely. Furthermore, in motor-driven systems, AVRs regulate essential parameters like torque and speed for optimal performance. By eliminating energy waste and enhancing reliability of the system, AVRs foster the long-term sustainability of the power grid and the related industrial machines while contributing to making the electrical infrastructure more cost-effective. However, despite their widely recognized advantages, AVRs constantly struggle to adjust the fluctuations in dynamic loads, which makes their development of complex control strategies necessary to improve their functionality and resilience in a range of operating environments [1], [2].

To effectively manipulate the voltage in a variety of load conditions, various control techniques have been proposed, ranging from conventional Proportional-Integral-Derivative (PID) controllers to more advanced approaches. PID controllers are utilized extensively in AVR systems because of their affordable, simpler to use, and flexibility in both linear and nonlinear systems. The controller itself is made up of three parts: the derivative term, which forecasts future error trends; the integral term, which corrects for accumulated previous errors; and the proportional term, which modifies output according to the current error [3]. Despite their widespread application, PID controllers frequently have tuning issues since traditional methods are used like "trial and error," Cohen-Coon, and Ziegler-Nichols [4], [5] techniques might not always offer optimal performance, resulting in overshoot or system instability. In response, researchers investigated several Artificial Intelligence (AI) methods, such as Fuzzy Logic (FL) [6] and Artificial Neural Networks (ANN) [7], for optimizing PID controller parameters. However, these techniques can be computationally costly and time-consuming. The limitations of conventional procedures and artificial intelligence techniques have led to the development of advanced methods for optimization for improving PID controller performance.

As a result, different optimization techniques were afterwards introduced that modify the PID controller in AVR systems. Three primary groups of optimization strategies have been identified by researchers [8], including physics-based, swarm-based, and evolution-based methods. Evolutionary optimization methods, such as Genetic Algorithms (GA) [9], Simulated Annealing (SA) [10], Differential Evolution (DE) [11], and Nondominated Sorting Genetic Algorithm II (NSGA-II) [12], have grown widely recognized for their effectiveness in simulating natural selection processes to enhance PID controller performance. In addition to evolutionary methods, swarm-based optimization [13] uses swarm intelligence, inspired by the collaborative behavior of bees, ants, and birds, PID controllers are used to identify the best solutions for AVR systems. Particle Swarm optimization (PSO) [14], proposed by Gaing et al. in 2004, presents itself as an effective tool for PID adjustments and quick, accurate optimizations in consistent voltage regulations since it converges more quickly and has greater global search capabilities than GA. By optimizing PID parameters, Sikander et al. (2018) created the Cuckoo Search Algorithm (CS) [15], which enhances system accuracy, dynamic response, and stability. Additionally, In AVR systems, Crazy PSO (CRPSO) [16] modifies PID parameters for more adaptable and reliable operation. Other swarm-based techniques have also been successfully implemented in AVR systems, including Ant Colony Optimization (ACO) [17] and Artificial Bee Colony (ABC) [18]. Swarm-based techniques are still being used to solve nonlinear PID optimization problems" In order to maximize AVR parameters and increase search efficiency, the CAS technique [19] integrated swarm intelligence with chaotic dynamics in 2015. The Ant Lion Optimizer (ALO) [20] optimizes real-time PID modifications by leveraging chaotic interactions and gravity forces.

However, physics-based optimization [21] has enhanced PID controller performance in AVR systems [22] by employing natural laws like chaotic dynamics and gravitational forces. The Gravitational Search Algorithm (GSA) [23], which is based on Newton's law of gravitation, is very

good in determining the best PID parameters and optimizing nonlinear systems. Complex solution spaces in nonlinear systems can be solved and local minima avoided with the assistance of chaotic systems, such as those that employ the Luozi map-based Chaotic Optimization [24]. Although these techniques have greatly increased the AVR systems' stability and performance [30], they have drawbacks, particularly in complex systems, such as premature convergence and local optima. To address these issues, the Sine Cosine Algorithm (SCA) [25], which Mirjalili introduced in 2016, has been utilized in AVR optimization system, to improve system dynamics by establishing a balance between exploration and exploitation. However, it still faces challenges because of complicated algorithmic architecture and occasionally problematic outcomes. To further improve AVR regulation, the NSCA-SPID (Nonlinear Sine-Cosine Algorithm-based Sigmoid PID) [26] controller was presented in 2018 by Suid et al. with the goal of maximizing system performance. However, a limitation in the performance of AVR systems emerged when complexity caused the step-response performance to decrease. To enhance system performance and offer a simple yet effective modify for practical AVR issues in unknown configuration spaces, the study in 2024 integrated amplifier feedback dynamic weighted (AFDW) [27] technique to the 1DOF PID control framework. According to research, many controllers in literature employ traditional PID structures, which need to be critically examined to improve system performance. Although the Sliding Mode [28], chattering may cause mechanical failure, PID controllers improve AVR reliability and interruption rejection by combining sliding mode control (SMC) [29] with PD control. Although they may exhibit lower accuracy, grey PID (GPID) [30] controllers manage systems with less data. Although fuzzy logic PID (FLCPID) controllers [31] dynamically adjust system parameters, heuristic tuning may cause performance variations. In high-mass systems, sustained disturbances can lead to instability, whereas the PIDA controller [32] reacts rapidly to changes in load. Although Sigmoid PID (SPID) [33] minimizes overshoot, it must be carefully adjusted when input varies quickly. Advanced PID controllers that only have one degree of freedom (1 DOF) increase responsiveness and decrease instability but introduce complexity, which compromises accurate performance. In AVR systems, feedback from both the generator and amplifier is combined via sensor tracking [34], improving system robustness. Research in [27] shows that feedback weighting enhances system dynamics performance.

Despite, the previously examined literature having accomplished its stated goals, there are several significant issues that must be addressed to ensure future advancement. Modern methods for optimization continue to encounter challenges such local optimal solutions, restricted progress, and premature convergence. These problems are mostly caused by an imbalance between exploration and exploitation tactics [35]. When traditional PID controllers with fixed coefficients are used, the AVR system frequently encounters operational difficulties. To overcome these challenges, A NSCA-SPID (Nonlinear Sine-Cosine Algorithm-based Sigmoid PID) controller must be implemented. Researchers have effectively implemented dynamic feedback weighting in 1-DOF controller configurations through sensor gain modifications, greatly improving control engineering performance and stability. There is still a gap in the use of the Sigmoid PID controller with amplifier feedback dynamic weighting (AFDW) in a 1DOF system, even though numerous optimization strategies have been developed for PID controllers in AVR systems. For the first time, the NSCA-SPID controller with AFDW is presented in this work, offering a more reliable and precise method of voltage regulation in AVR systems. The research evaluates the superiority of the NSCA-SPID controller by comparing it with various PID-based controllers such as hVSAGWO, VSA-PID, GWO-PID, and SCA-PID. The study employs quantitative analysis using time response criteria and the Figure of Demerit (FOD) to validate the efficacy of the proposed method. To verify the effectiveness of the suggested approach, the study uses quantitative analysis with time response criteria and the Figure of Demerit (FOD). The primary contributions of this study consist of.

1. The NSCA-SPID controller was successfully implemented for the first time with an amplifier feedback dynamic weighted approach (AFDW) system.
2. Second, the superiority of NSCA-SPID was evaluated in comparison to other recently developed approaches, including VSAGWO, VSA-PID, GWO-PID, and SCA-PID.

Subsequently, the current article's remaining content is arranged as follows: The AVR system is described in Section 2. Section 3 gives a thorough overview of the several AVR controllers, while Section 4 explains how the SPID controller of the AVR system self-tunes. The simulation results are shown in Section 5. Lastly, Section 6 provides a summary of the study's findings.

2. Description of an AVR System

The AVR system's main functionality is to maintain the output voltage of the generator within a prescribed range, consider fluctuations in the load, and keep the system stable. Its function is to identify fluctuations due to changing loads and regulate the generator's terminal voltage to maintain power quality. The amplifier compares the terminal voltage to the reference voltage, and a voltage feedback sensor measures the resultant change. Using the error signal, the exciter amplifies or attenuates the excitation to produce or depress the voltage gain to maintain the terminal voltage or stable power quality [6]. In Fig. 1, we present an overview of the fundamental AVR system.

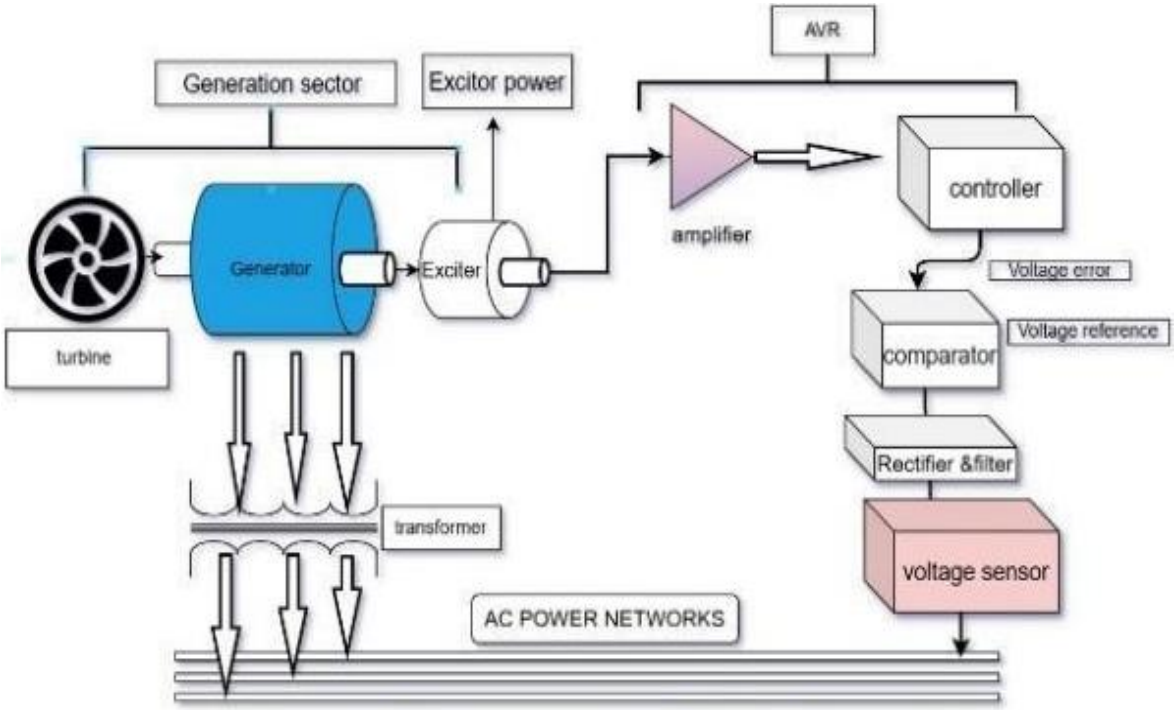

Fig. 1. Controlled AVR system arrangement [27]

In the conventional approach, the generator's outputs are monitored by a sensor. An error signal is generated as the controller's input following a comparison of the sensor's output with the reference voltage value. In addition, a sensor that tracks generator and amplifier feedback has been integrated into an amplifier feedback system. To get the controller input, these two feedback signals are combined and compared to the reference voltage level. This method makes the system's response to AVR more reliable. This approach's greater impact is demonstrated in [20]. This study also considers dynamic weighting of the feedback by varying the sensor gains for the 1-dof controller. The constraints of the IEEE standard for the DC1C excitation model and [27] are also taken into account in order to calculate near-real AVR performances. The non-linear AVR system's basic model with AFDW is shown in Fig. 2.

In Fig. 2, the symbols, K_e, and K_g indicate generator gain, exciter gain, and amplifier gain, respectively. Likewise, the symbols for the amplifier, exciter, generator, sensor 1, and sensor 2 denote their respective time constants, T_a, T_e, K_g. The range of AVR settings mentioned in the literature [27] is shown in Table 1:

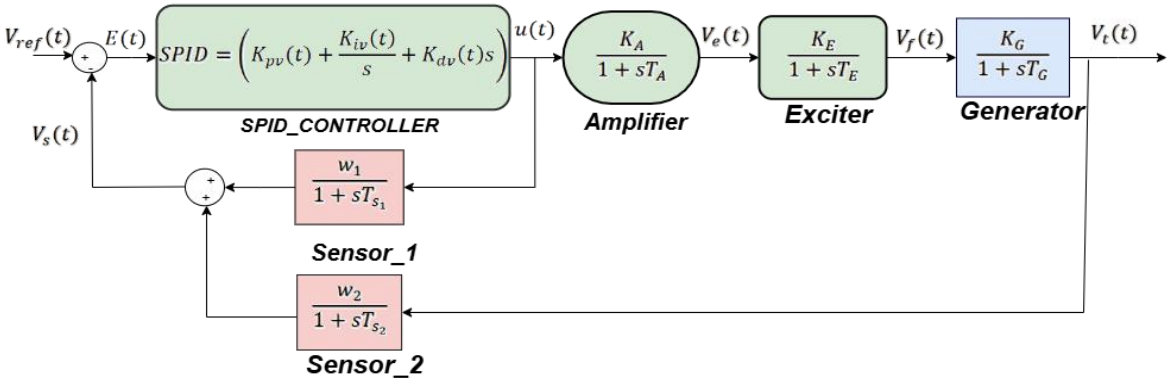

Fig. 2. Proposed non-linear AVR model having AFDW [27]

Table 1. Parameter limits of the non-linear AVR model with AFDW

AVR Component	Parameter Limit	Parameter Values in AVR System
Sensor	$0.001 \leq T_{s1}, T_{s2} \leq 0.006$ $0 \leq w_1, w_2 \leq 1$	T_{s1}= 0.01, T_{s2}= 0.01
Generator	$1.0 \leq T_g \leq 2.0$ $0.7 \leq K_g \leq 1.0$	T_g = 1 K_g = 1
Exciter	$0.4 \leq T_e \leq 1.0$ $1.0 \leq K_e \leq 10$	T_e = 0.4 K_e = 1
Amplifier	$0.02 \leq T_a \leq 0.1$ $10 \leq K_a \leq 400$	T_a = 0.1 K_a= 10
PID controller	$0.2 \leq K_p, K_i, K_d \leq 2.0$	K_p, K_i, K_d = optimized values

The dynamic weighted coefficients of the sensors used in this work, w_1. and w_2, are given in Eq. (2) and chosen from [0,1]. The dynamic weighted coefficient total, which is provided, is also assumed to be 1.

$$0 \leq w_1, w_2 \leq 1 \tag{1}$$

$$w_1 + w_2 = 1 \tag{2}$$

Fig. 2 illustrates how the dynamic weighted uncontrolled non-linear AVR system is impacted by the proposed AFDW approach. The system response is less varied when employing an AFDW approach than when using one, as seen in Fig. 2. In contrast, the AFDW approach was favorably received by the uncontrolled system. consistent with the conventional approach. Uncontrolled AVR systems' performance is also greatly impacted by the AFDW approach.

3. Controller of AVR System

In the following section, the Sigmoid PID (SPID) controller, an advanced family of PID control techniques, is investigated. First, The SPID controller's fundamental idea will be explained, along with its benefits and drawbacks. After that, the newly proposed SPID control method's working concept is explained. While controlling the AVR system, it is expected to offer better performance precision control.

3.1. PID Controller

In the section that follows the structure of the PID controller in closed-loop cellular vehicle control will be illustrated along with how to fix the AVR terminal voltage at the maximum level allowed. In addition, the original PID's strengths and limitations are first examined to identify elements that are viable to be improved [36]. A suitable mathematical description of the AVR system

is required to explain the PID controller of the system. All the AVR system elements, i.e., the exciter, sensor, amplifier, and generator, may be linearized to achieve the goal. The transfer functions of the PID controller and all the previously listed components are shown in Fig. 2. It is mentioned that this AVR model is widely utilized through writing, and the preferred parameter settings for the system are presented. The values in this paper were the same as those reported in [37]. Consequently, each component is linearized using a gain and a time constant to prevent saturation or other nonlinearities. The foundation of the controlled AVR system is the error detection idea.

$$K_{pv}(t) = K_{plo} - \left| \frac{K_{phi} - K_{plo}}{1 + e^{-\sigma_p |\Delta v_e(t)|}} \right| \tag{3}$$

$$K_{iv}(t) = K_{ilo} - \left| \frac{K_{ihi} - K_{ilo}}{1 + e^{-\sigma_i |\Delta v_e(t)|}} \right| \tag{4}$$

$$K_{dv}(t) = K_{dlo} - \left| \frac{K_{dhi} - K_{dlo}}{1 + e^{-\sigma_d |\Delta v_e(t)|}} \right| \tag{5}$$

$$SPID = \left(K_{pv}(t) + \frac{K_{iv}(t)}{s} + K_{dv}(t)s \right) \tag{6}$$

In particular, K_{phi}, K_{ihi}, *and* K_{dhi}, are the upper bounds and K_{plo}, K_{ilo} , K_{dlo}, are the lower bounds of SPID controller settings in Eq. (3)-(5). However, each gain in the traditional PID controller serves multiple purposes, including controlling the speed of the response's speed utilizing K_p gain such that a higher K_p gain will decrease the rise time, K_i gain with the aim to eliminate the steady-state inaccuracy. and K_d gain will enhance the output of the transient response and have an impact on the overshoot. However, a greater K_d parameter may make the control system react to changes in error signals with greater force. Next, it will use the upper and lower bounds in order to provide an optimal PID gain border as in $K_{pv}(t)$, $K_{iv}(t)$, and $K_{dv}(t)$ such that the response's speed, steady state, and transient are all substantially improved [11]. Furthermore, if the gain values are constrained by such an error signal from the standpoint of the upper and lower values of the gain, then an appropriate controller signal $u(t)$ can be originated. Furthermore, the constants σ_p, σ_i, σ_d are included to modify how steeply the top and lower bounds transition; and $V_e(t)$ is a function of error between the synchronous and sensor voltages. It should be noted that the $K_{pv}(t)$, $K_{iv}(t)$ and $K_{dv}(t)$ in Eq. (3)-(5) are varied in terms of the error signal and alternate. Unique values of the curve sharpness σ_P, σ_i, σ_d, are taken for each $K_{pv}(t)$, $K_{iv}(t)$ and $K_{dv}(t)$. These values do not constrain the error signal in any way. To design of parameter tuning, we define $\Delta_p = | K_{phi} - K_{plo}|$, $\Delta_i = | K_{ihi} - K_{ilo}|$, and $\Delta_d = | K_{dhi} - K_{dlo}|$.

4. Self-Tuning SPID Controller of AVR System

This segment explains the original SCA optimizer through an analysis of its beneficial features and potential areas that need improvement. Its rules are based on simple sine and trigonometric cosine functions. SCA optimization algorithms and their enhanced variants are implemented in a variety of real-world engineering applications to address issues such as grid-integrated solar systems, energy storage systems, rotating equipment fault diagnostics, and hydropower reservoir operation optimization [38]. As with other multi-agent-based optimization techniques, SCA's initial exploration process uses one or more sets of search agents to conduct its value search. The following issues are addressed by search agents that are both generated and deployed at randomly throughout designated optimization areas.

$$arg \min_{X_j(1), X_j(2), \ldots} f_j(X_j(k)) \tag{7}$$

Where f_j is the agent's primary function and X_j is an agent that uses position vector j. The algorithm then notes that these positions are the most optimal it has ever seen and identifies them as the desired point. The optimization process will continue until the maximum value is reached, at which point it will stop. The sine and cosine functions are used to update each agent's position as follows:

$$X_{ij}(k+1) = X_{ij}(k) + r_1 \cdot \sin(r_2) \cdot \left| r_3 P_i - X_{ij}(k) \right| \tag{8}$$

$$X_{ij}(k+1) = X_{ij}(k) + r_1 \cdot \cos(r_2) \cdot \left| r_3 P_i - X_{ij}(k) \right| \tag{9}$$

The symbol for the iterations $k = 0, 1, 2, \ldots$ is $X_{ij}(k)$. It shows where the agent is at the moment. For $i = 1, 2, \ldots d$, P_i is ultimate location in the ith dimension, and j in the ith dimension. To keep things simple, P_i is the destination position vector, or the best solution that was found at the time. Then, these two equations are put together as follows:

$$X_{ij}(k+1) = \begin{cases} X_{ij}(k) + r_1 \cdot sin(r_2) \cdot \left| r_3 P_i - X_{ij}(k) \right|, if\ r4 < 0.5, \\ X_{ij}(k) + r_1 \cdot cos(r_2) \cdot \left| r_3 P_i - X_{ij}(k) \right|, if\ r4 \geq 0.5, \end{cases} \tag{10}$$

Where r_2, r_3, and r_4 are the crucial parameters in SCA which are random in nature and || indicates the actual magnitude value operation being carried out. The parameter r_2 represent the position motion's distance toward or approach to the destination position, which is randomly generated in [0, 2π]. The target position's random weight, r_3, is randomly selected in [0, 2] so that it either systematically increases ($r_3 > 1$) or decreases ($r_3 < 1$) the distance to the present location. The functions of the sine and cosine in Eq. (10) are randomly alternated from the parameter r_4 [13]. The parameter r_4 is randomized between [0,1]. The equations above make it clear that parameter r_1 is the following position, which, determined by one of the key coefficients, might just be the exploration or exploitation stage [14]. To maintain the equilibrium between these two exploration and exploitation skills, the equation r_1 is given by:

$$r_1 = a - k\left(\frac{a}{K_{max}}\right) \tag{11}$$

Where K_{max} is the greatest iterations, a constant, that are currently taking place. In simple terms, the SCA method will investigate the global search area when $r_1 > 1$. If not, when $r_1 \leq 1$, The local search area will be used by the SCA. The study in [39] proved the effectiveness of SCA compared to other competitive algorithms. Notwithstanding reports that the SCA was effective in resolving the AVR issues, several instances of system high overshoot and slow settling time were observed. In practical terms, these drawbacks are mostly due to the position updated Eq. (11), which openly destabilized the accuracy of the answer by using a linear declining approach. Flowchart of NSCA_SPID shown in Fig. 3.

4.1. Overview of Sine Cosine Algorithm (SCA)

This phase provides an extensive overview of the original SCA optimizer in order to evaluate its strengths and potential areas for improvement. Basic sine and cosine trigonometric functions serve as the optimization criteria for SCA, which operates via a multi-agent approach. Together with its other improved versions, the SCA serves as a problem-solving tool for real-world engineering applications such as energy storage systems, grid-integrated photovoltaic systems, rotating machinery fault diagnosis, and hydropower reservoir operation optimization [25]. In order to find optimal values, the SCA search method uses sets of exploratory agents, just like other multi-agent-based optimization strategies. Agents in the predefined search region are positioned at random to solve optimization problems, such as the following:

4.2. Nonlinear Sine Cosine Algorithm (NSCA)

The current section explores the proposed Nonlinear Sine Cosine Algorithm (NSCA), which demonstrates how it improves both the exploration and exploitation capabilities of the basic SCA approach. The first implementation of SCA used 50% of iterations for both exploration and exploitation phases. A theoretical dichotomy exists between exploration and exploitation because advancing one aspect automatically causes the deterioration of the other [40]. The algorithm loses its ability to determine the exact overall optimal values when exploration exceeds the optimal threshold. An unsatisfactory estimated value emerged from excessive exploitation because it decreased the possibility of avoiding being stuck at a local optimal point. During this optimization method, the SCA used parameter r_1 in Eq. (11) to follow a linear reduction pattern from 2 to 0). The present equation only provides limited applications for SCA, but experts acknowledge the need for a more extensive r_1 formula that would suit multiple usage scenarios [41]-[46]. The exploration and exploitation phases are beyond the user's control, which results in significant limitations in the current r_1 system. Then a declining nonlinear curve based on the exponential function became the selection for Eq. (11). Consequently, equation of r_1 in Eq. (11) is revised as:

$$\hat{r}_1 = a\left(1-\left(\frac{k}{K_{max}}\right)^{\alpha}\right)^{\beta} \tag{12}$$

The new nonlinear conversion indexes β and α illustrate the two parameters in the equation. The non-linear conversion indexes β and α controlled the proportion of exploitation to exploration during the tuning process.

Therefore, in the suggested NSCA approach, the established version of Eq. (11), was replaced with the new $\hat{r}_1$ in Eq. (12). By setting β = 1.0 to values of α > 1.0, β < 1.0, or β > 1.0 and α = 1.0, for instance, the method was supposed to have a significant capacity for exploitation. When the parameters β and α fell between [0.1, 0.3] and [0.02, 0.04], respectively, the NSCA technique might yield the best outcomes, according to the study reported in [47]. Despite only avoiding the local trapped situation, the reasoning behind these defined values was taken into account to speed up convergence. According to estimates, applying NSCA optimization in the AVR application may result in an enhanced transient response profile with quicker settling times, less voltage overshoot, and the least amount of steady-state error. The pseudocode for the recently proposed NSCA method is shown in Fig. 4.

4.3. The Application of the Proposed NSCA for SPID Controller Tuning of AVR System

The following part describes how to install the suggested NSCA-tuned SPID controller to improve the AVR system's response. determining the SPID controller parameters' ideal values to allow the controlled system to attain an exceptional degree of accuracy in control performance was one of the main objectives of the NSCA technique. Similar to [48] and [49], this study also considered the Figure of Demerit (FOD), which is an objective function of response specification that varies over time. This is the expression for the FOD objective function.

$$FOD = (1 - e^{-\gamma})(M_p + E_{SS}) + e^{-\gamma}(T_S - T_r) \tag{13}$$

In Eq. (13), M_p, E_{ss}, T_{set}, and T_r are employed to depict the various components of the time response specification, including overshoot, rising time, settling time, and steady state error, accordingly. The value of γ in Eq. (13), should be taken into consideration and should also be changeable together with a system's requirements. For example, set γ can be assigned to be greater than 0.7, when M_p, and E_{ss} do not have to be at a low level. On the other hand, if the value of γ was less than 0.7, the T_r and T_s values might be able to decrease. The value of γ in this work was set 1.0, the same as the values reported in [50] and [51].

Problem 4.1:

Utilizing the implementation of the block diagram of the proposed non-linear AVR model having AFDW shown in Fig. 2, find the ideal values for the SPID gains, i.e., K_{pv}, K_{iv}, K_{dv}, such that the performance index FOD is minimized.

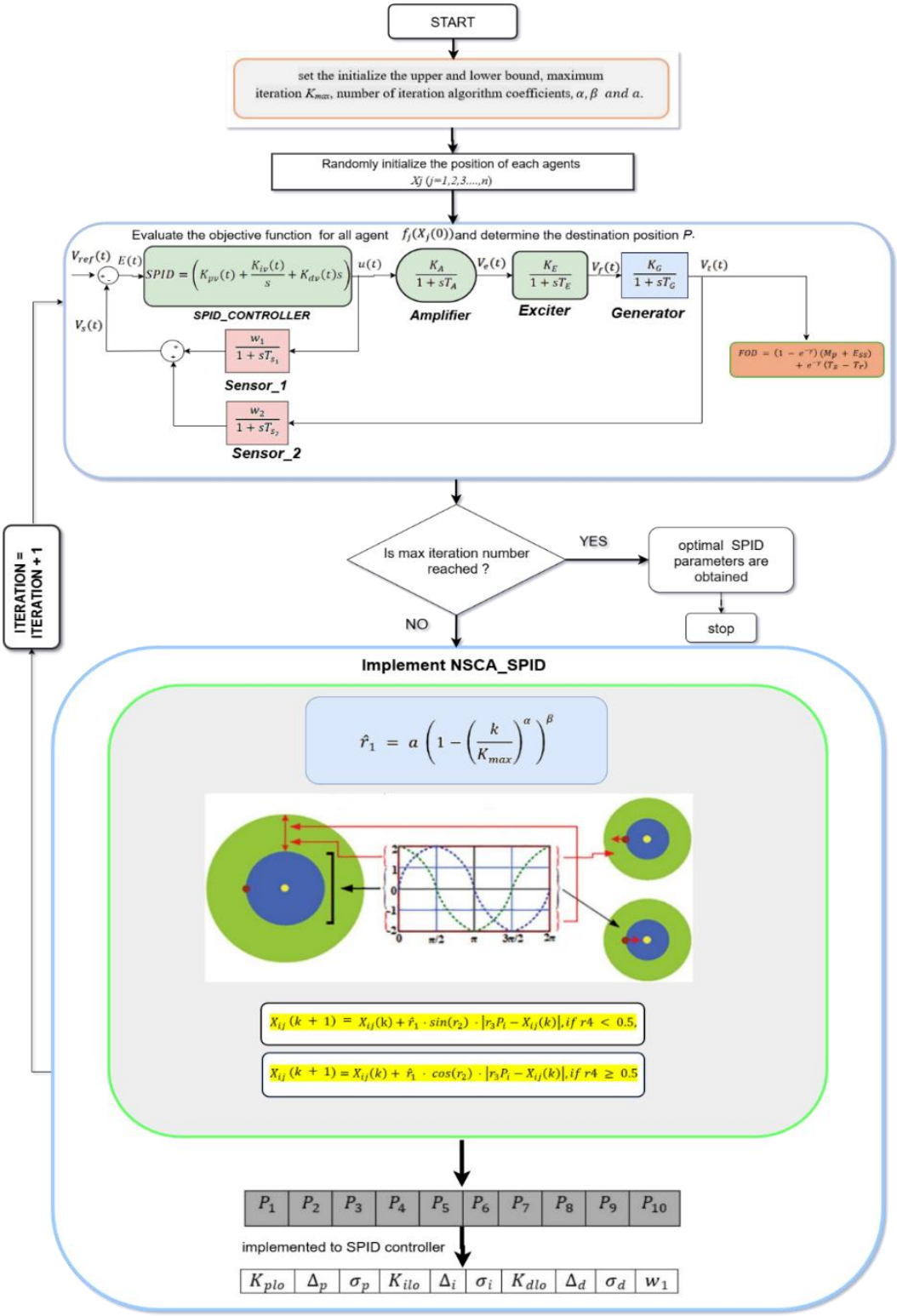

Fig. 3. Flowchart of NSCA_SPID

It is noted that FOD uses just one objective function. The main features of FOD are these. To begin with, FOD handles a more modest control objective function because the FOD arrangement

itself gives times identical weights (T_{set} and T_r) and amplitudes (M_p and E_{ss}). In contrast, the sum of timings and amplitudes is subjected to exponential weights. Consequently, the FOD that is produced can surely depict the reaction properties of the AVR system. Second, FOD uses just one coefficient to sufficiently satisfy the designer's needs, while many other articles need a great deal of work to determine the appropriate value of numerous weightages in their objective function. (i.e., γ) [52]. Meanwhile, the multi-objective function presented in [53], [54] can offer good performance, but because the number of optimizations runs increases exponentially with all the objectives, it typically requires a lot of computer resources to identify the Pareto front.

AVR systems with the suggested NSCA-SPID controller are generally arranged in Fig. 5. The first step in using the NSCA optimizer to optimize the SPID controller parameters is to assign the agent position vector in Eq. (7) is mapped with the ten design parameters in Eqs. (3)-(5) as $X_j(k) = [\, K_{plo}, \Delta_p, \sigma_p, K_{ilo}, \Delta_i, \sigma_i, K_{dlo}, \Delta_d, \sigma_d, w_1]$ at the same time, the FOD function in Eq. (13) has been assigned to the objective function f_j in Eq. (7) as f_j = FOD.

Algorithm 1: Proposed NSCA Algorithm

1. Set the initial parameters setting upper bound (ub) and lower bound (lb), maximum iterations number (K_{max}), number of agent (n) and coeffecients α, β *and* a
2. Randomly initialize the position of each agent $X_j(j = 1, 2, 3, \ldots, n)$
3. Evaluate the objective function of all agents $f_j(X_j(0))$ and determine the destination position $\boldsymbol{P}$.
4. ***for*** $k = 1: K_{max}$
5. update $\hat{r}_1$ using Eq. (12)
6. ***for*** $i = 1: d$
7. ***for*** $j = 1: n$
8. generate random numbers r_2, r_3, r_4 independently
9. obtain the updated position $X_{ij}(k+1)$ using Eq. (10)
10. ***end for***
11. ***end for***
12. evaluate the objective function $f_j(X_j(k+1))$
13. ***if*** $f_j(X_j(k+1)) < f(\boldsymbol{P})$
14. $\boldsymbol{P} = X_j(k+1)$
15. ***end if***
16. ***end for***
17. Return $\boldsymbol{P}$ best solution obtained so far

Fig. 4. Pseudocode of the proposed NSCA optimization algorithm [26]

In theory, the NSCA method minimizes the value of the objective function f_j to maximize the agent position $X_j(k)$. The E_{ss}, M_p, T_r, and T_{set} values are represented by distinct j values that are produced by each $X_j(k)$ in the suggested technique. The best f_j values and their matching position vector $X_j(k)$, which is also known as the destination position P, are then determined by ranking each f_j. Next, using Eq. (12), the agent location $X_j(k)$ is adjusted. This is in line with the SPID controller's updated tuning value at the following iteration. This duplex coordination between the NSCA optimizer and the SPID of the AVR system is executed recursively till the end. The following is a summary of the NSCA's comprehensive procedure for modifying the SPID controller of the AVR system:

- (Step 1): Determine the sigmoid PID controller parameters' upper and lower bounds (u_b) and (l_b), then initialize the search agents' and destination position P at random. Indicate the maximum number of iterations, K_{max}, as well as the coefficients β and α.
- (Step 2): Calculate f_j $(X_j(k))$ of each agent j by setting f_j $(X_j(k))$ = FOD (K_{plo}, Δ_p, $\sigma_p, K_{ilo}, \Delta_i, \sigma_i, K_{dlo}, \Delta_d, \sigma_d, w_1$).
- (Step 3): Determine each agent's associated position vector, or destination position $\boldsymbol{P}$, by finding the minimum f_j $(X_j(k))$.
- (Step 4): Construct $\hat{r}_1$, in Eq. (12) and random variables r_2, r_3, r_4.
- (Step 5): Using the new $\hat{r}_1$, update the position using Eq. (10).
- (Step 6): Proceed to Step 7 if the number of iterations reaches the maximum value K_{max}. Otherwise, go back to Step 2.
- (Step 7): The optimal controller parameter is denoted by the value P that yields the lowest value of FOD.

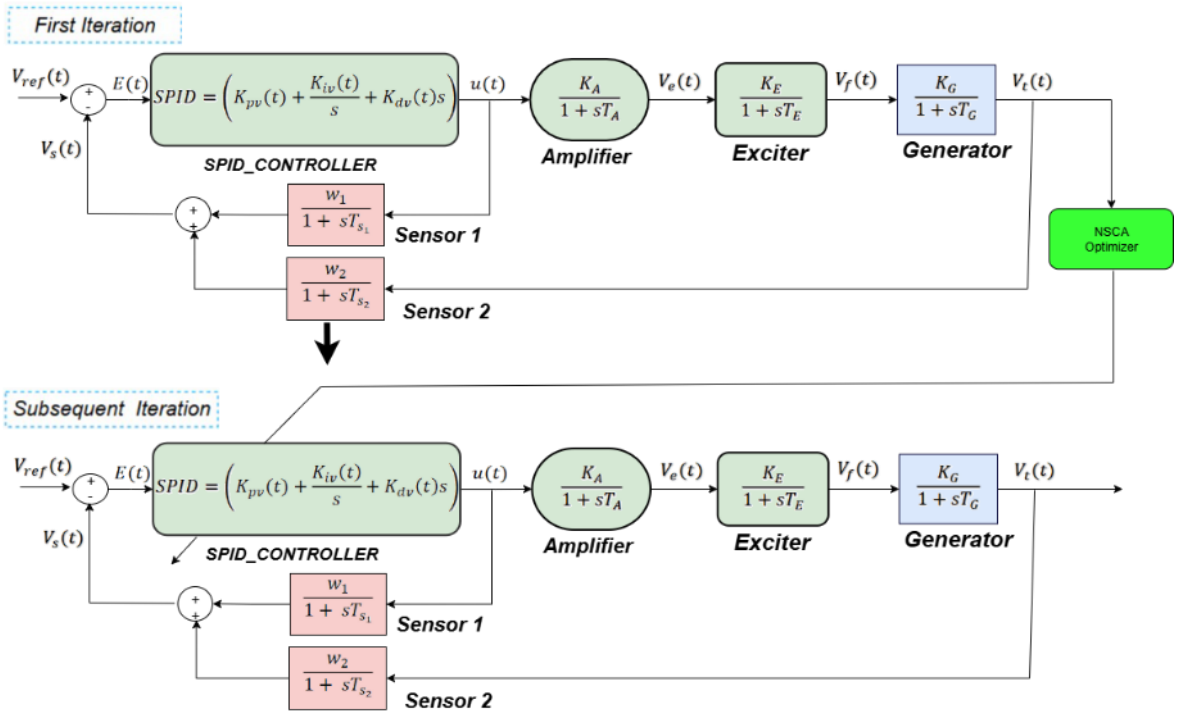

Fig. 5. AVR system with NSCA-SPID controller

The NSCA-SPID controller can be used to the real AVR system in the following ways. First, using the system identification technique, the AVR system model is acquired. Second, in the simulation environment (i.e., offline mode), the NSCA technique is used to develop and tune the SPID controller for the acquired AVR model. Following the acquisition of the ideal SPID parameters, the microcontroller that is integrated with the actual AVR system uploads those parameters to the SPID controller. Be aware that there have been reports of this type of framework in [55].

5. Simulation Results

The following part evaluated how well the proposed NSCA-SPID technique worked to maximize AVR system performance. A comparison was made with other techniques like hVSAGWO, VSA-PID, GWO- PID, SCA-PID and proposed NSCA-SPID to assess its ability to improve the AVR

system efficiency. The performance of each method was evaluated according to the following criteria: The measurement of time response specifications and the precision of FOD, as described in Eq. (13). number of objectives. The regular arrangement of an AVR system using the suggested NSCA-SPID controller can be seen in Fig. 6. For optimizing the SPID controller parameters using NSCA optimizer, firstly, Eq. (3)-(5) relate the 10 design parameters to the agent position vector as $X_j(k)$ =[K_{plo}, Δ_p, $\sigma_p, K_{ilo}, \Delta_i, \sigma_i, K_{dlo}, \Delta_d, \sigma_d, w_1$]. Meanwhile, the FOD function in Eq. (13) is mapped to the objective function f_j in Eq. (7), with f_j = FOD. In theory, the NSCA method reduces the goal function's value. From a technical standpoint, the NSCA technique maximizes the agent position, $X_j(k)$. by minimizing the value of the objective function, f_j. Technically, the NSCA technique minimizes the value of the objective function, $X_j(k)$, in order to optimize the agent position $X_j(k)$. In the proposed method, each $X_j(k)$ produces different f_j values which correspond to the E_{ss}, M_p, T_r, and T_{set} values.

This study uses a laptop equipped with a 2.8 GHz Intel® Core i5 processor and 12 GB of RAM, employing MATLAB/Simulink version 9.12.0.1884302 (R2022a) for the simulation. In the proposed NSCA implementations, the population size, defined as the number of agents, was established at 30, whereas 50 iterations were set as the maximum number. For a fair and comparable assessment, it is crucial to note that this scenario was utilized in another study [56]. The coefficients of the proposed NSCA were determined to use a = 2, β = 0.3, and α = 0.03. The proposed control parameters were established with a l_b of 0.2 and u_b of 20.

To improve the search area for optimal results, the suggested NSCA methodology uses wider ranges of u_b. and l_b values (i.e; u_b = 2.0 and, l_b = 0.2). The choice of, u_b = 0.2 was comparable to the research in [57] and [58]. Nevertheless, the calculation of u_b = 20.0 was predicted on preliminary tests that included recently added design components were used to evaluate the performance of each method.

1. The evaluation of the FOD's accuracy and time response specifications, as stated in Eq. (13).
2. The box plot and Wilcoxon's signed-rank are the fundamentals of the nonparametric statistical test.
3. The investigation of trajectory tracking in terms of *IAE*, *ISE*, *ITAE*, and *ITSE*, even in the event of disruption. The following is the mathematical expression for these performance metrics:

$$ISE = \int_0^{t_s} . \left(V_t - V_{ref}\right)^2 . dt \tag{14}$$

$$IAE = \int_0^{t_s} . \left|V_t - V_{ref}\right| . dt, \tag{15}$$

$$ITSE = \int_0^{t_s} . t\left(\left(V_t - V_{ref}\right)^2\right) . dt, \tag{16}$$

$$ITAE = \int_0^{t_s} . t\left|V_t - V_{ref}\right| . dt. \tag{17}$$

In equation (14)-(17), t_s is the final simulation time.

Additionally, the conventional PID controllers used for comparison are described in Table 2, along with their ideal gains. Moreover, a comparison of the terminal voltage step responses obtained

from each PID controller methodology is presented in Fig. 7. The SPID controller performs better than current multi-agent-based techniques, producing lower overshoot and more accurate and consistent terminal voltage step responses.

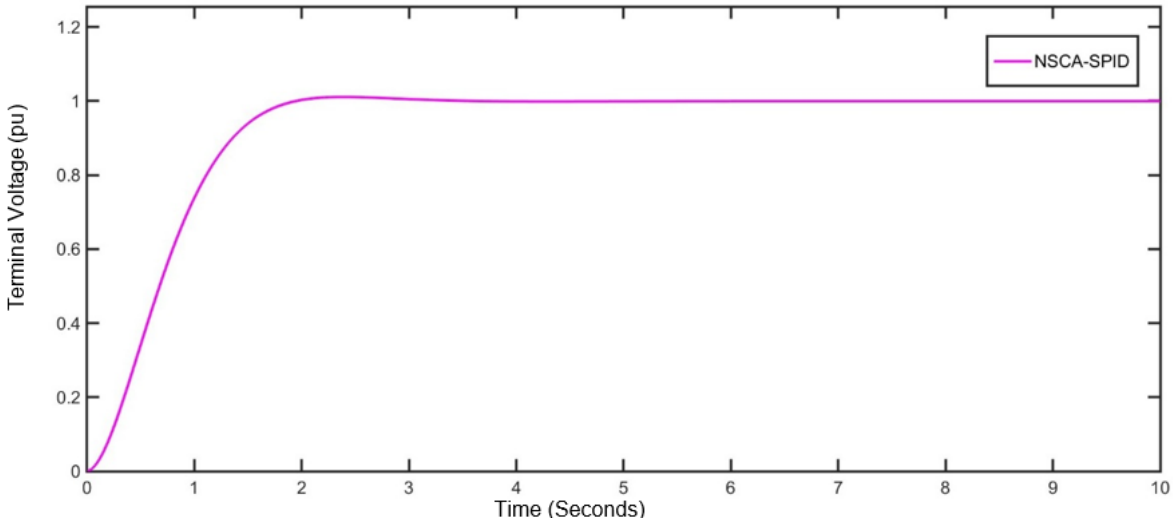

Fig. 6. Implementation of NSCA-SPID controller for AVR system

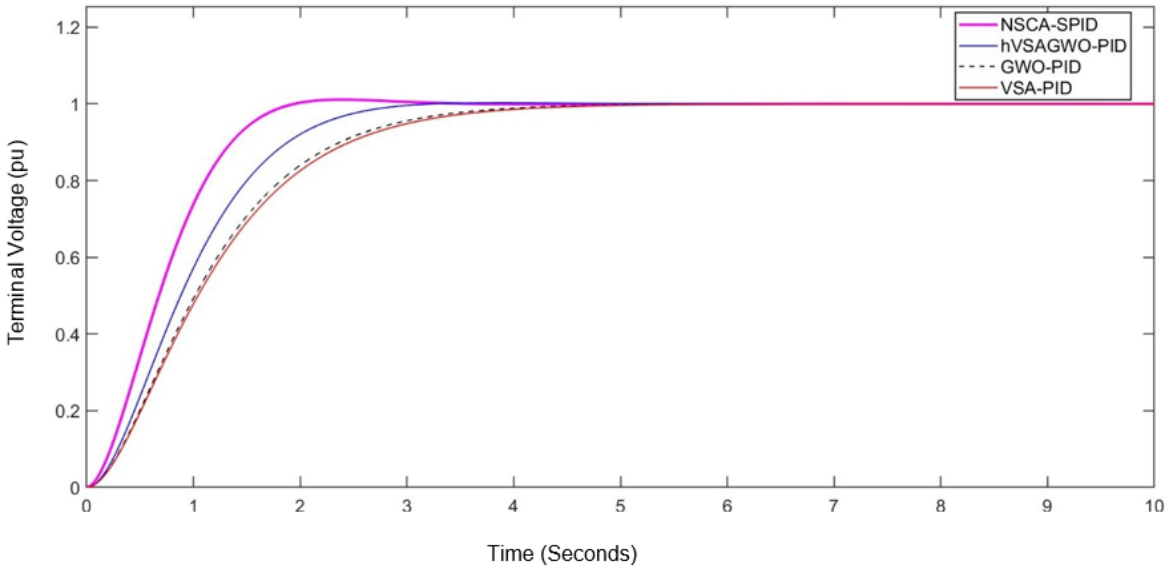

Fig. 7. The step responses of the AVR system produced by different metaheuristic-based controllers

5.1. Step Response Analysis

In this section, the trajectory tracking simulation was examined as the subsequent case study. The purpose of this analysis is to assess the correctness of the generated terminal voltage response by contrasting the NSCA-SPID controller with many newly released optimization-based PID controllers. The NSCA approach was used to track the target trajectory and change this. As illustrated in Fig. 8, our work focuses on monitoring the combination of ramp and step types of reference signal, in contrast to the earlier studies described in [59], [60] that used unit step as the input reference. To make things less difficult, to evaluate how well the proposed controller tracked the trajectory, the reference t input signal was placed in parallel with multiple set points (refer to Fig. 8). To ascertain the system, this inquiry is required.

The examination of the temporal response characteristics of the proposed SPID controller, which were modified using the NSCA technique, is presented in this subsection. As seen in Fig. 9, this

outcome was achieved by comparing the NSCA-SPID Controller with a number of recently released optimization-based PID controllers. Using the unit step as the input reference, modifications were performed to the implemented controllers. To evaluate the AVR system terminal voltage response's speed and steady-state inaccuracy, this analysis is required. When compared to other approaches, it is clear that the proposed NSCA-SPID controller can produce better response profiles by ensuring the most accurate (i.e., more accurate) and stable terminal voltage step response (i.e., less overshoot response).

During 50 iterations using the NSCA approach to provide the best optimized SPID controller parameters, as shown in Table 3 presents the design parameters, their associated tuned values, and their lower and upper bounds. Ten settings in all have been tuned to improve the system's performance. These parameters include precise weighting and scaling variables, as well as a variety of other aspects like proportional, integral, and derivative gains. Each parameter's values were carefully adjusted to provide the best possible system behavior within the predetermined parameters. Additionally, Fig. 10 shows the response of the objective function convergence. Additionally, Table 2 presents the optimal gain and settings of the controllers as well as information about conventional PID controllers that were used for comparison. Results of the FOD response specification shown in Table 4.

Furthermore, a statistical performance study was carried out on ten different experiments to evaluate the effectiveness of the suggested NSCA-SPID controller. We have compared the proposed NSCA-SPID with the current SCA-PID and two additional versions, NSCA-PID and SCA-SPID, which each adopt a part of the NSCA-SPID controller mechanism. A nonlinear statistical test called the Wilcoxon's signed-rank test was employed for evaluating how the methods and results differed; the results are displayed in Table 5. According to this table, S^+ is the sum of the ranks at which the first algorithm performed better than its competitor, while S^- is the opposite. With a significant level of 0.005859, the data clearly demonstrates that the suggested NSCA-SPID controller outperforms the SCA-PID controller.

In the meantime, a statistically significant difference between NSCA-SPID and two further NSCA-PID and SCA-SPID variants is also revealed by the comparison test results with p-value of 0.01934 and 0.009766, respectively. Furthermore, Fig. 11 graphically displays the box plot of the four controllers under comparison. It is clear that the present SCA-PID performed the worst across all performance criteria because it had the largest interquartile range. This suggests a poor level of consistency as a result. With the exception of the ITAE index, where the NSCA-SPID fared somewhat worse than the other two controllers, the results of the proposed NSCA-SPID were literally comparable to those of the NSCA-PID and SCA-SPID controllers. When it comes to precision, the NSCA-SPID is believed to perform competitively.

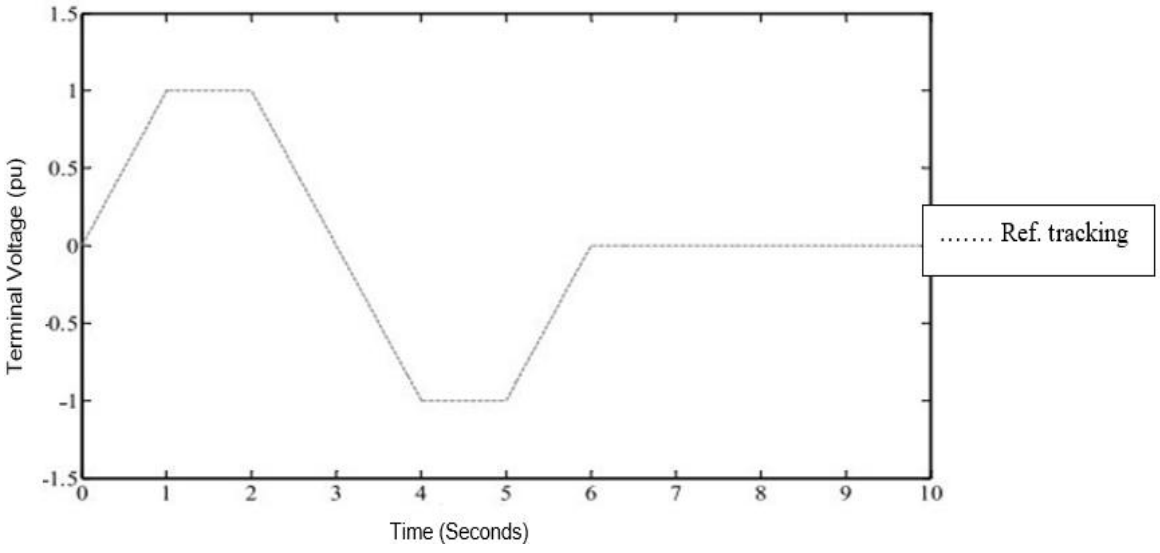

Fig. 8. Reference signal with various set points $V_{ref}(t)$

Table 2. Optimal settings of PID parameters

Algorithms	PID Controller's parameters			
	K_p	K_i	K_d	w_1
hVSAGWO-PID [27]	0.8300	0.9801	0.0201	0.6445
VSA-PID [26]	0.9091	0.9369	0.0230	0.8279
GWO-PID [4]	0.9900	0.9900	0.0100	0.8031
SCA-PID [25]	0.9900	0.9900	0.0100	0.8335

Table 3. Optimized design parameters of the proposed SPID controller

Design parameter	Lower bound	Upper bound	Tuned values
K_{plo}			14.22543
Δ_p			19.23791
σ_p			3.45565
K_{ilo}	0.2	20.0	6.42785
Δ_i			4.28271
σ_i			6.42785
K_{dlo}			9.99761
Δ_d			4.84982
σ_d			9.89244
w_1	0	1	0.51717

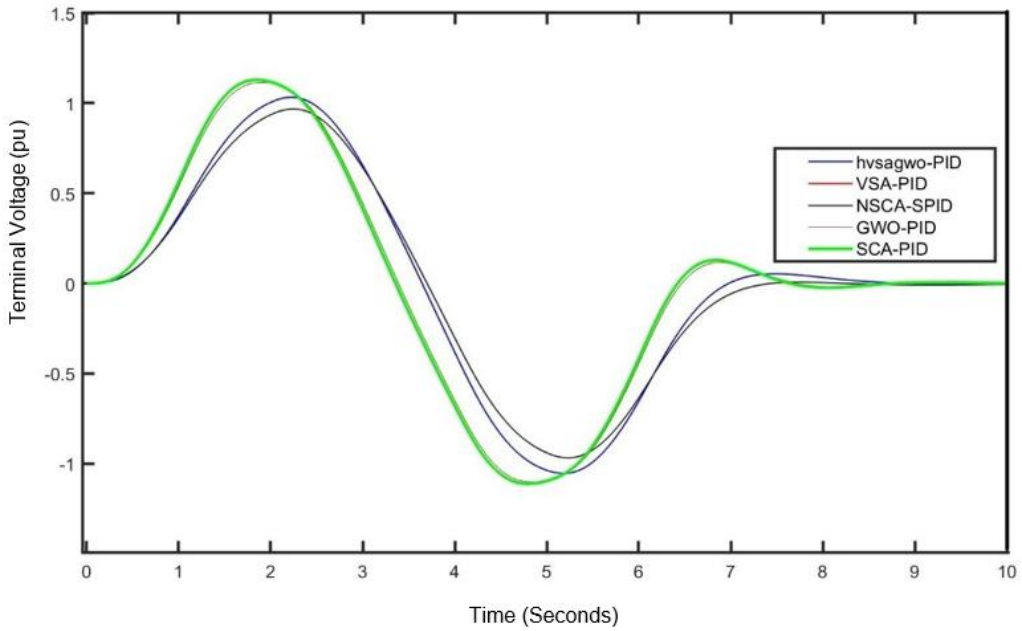

Fig. 9. Terminal voltage responses without any noise

Table 4. Results of the FOD response specification

Controllers	M_p	T_r	T_{set} (5%)	*FOD*
hVSAGWO-PID [27]	0.323	0.1586	2.923	0.5055
VSA-PID [26]	0.000	2.124	4.778	0.9814
GWO-PID [4]	0.000	2.052	4.603	0.9349
SCA-PID [25]	0.000	2.143	4.882	1.0015
Proposed NSCA-SPID	0.000	1.1475	1.9739	0.3064

Table 5. Wilcoxon's signed-rank analysis results for the 10 trails of FOD control performance

Controllers	S^+	S^-	p-value
Proposed NSCA-SPID vs NSCA-PID	52	3	0.009766
Proposed NSCA-SPID vs SCA-SPID	14	41	0.1934
Proposed NSCA-SPID vs SCA-PID	53	2	0.005859

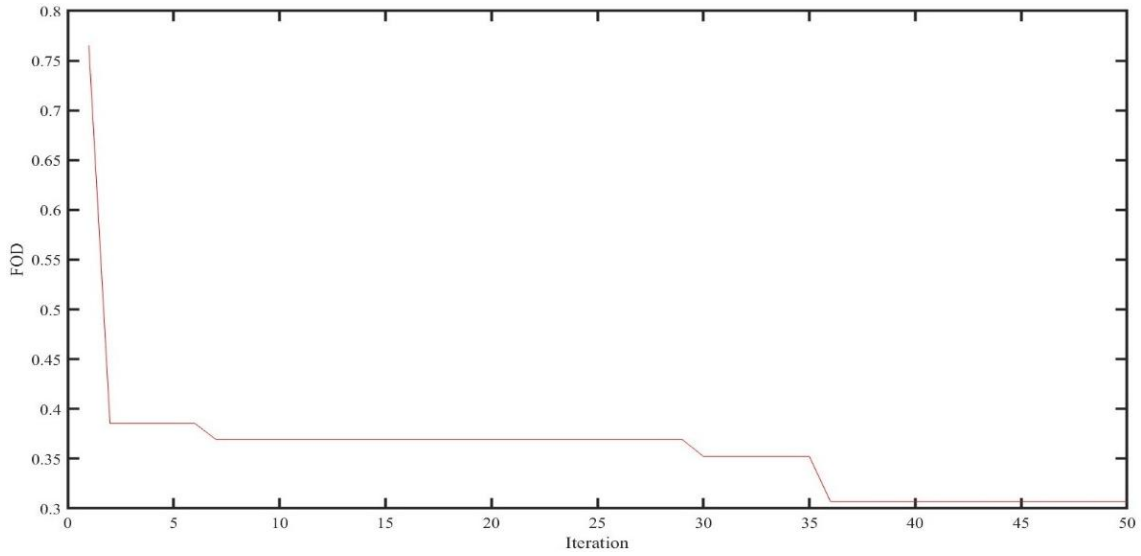

Fig. 10. Analysis of FOD convergence with NSCA algorithm

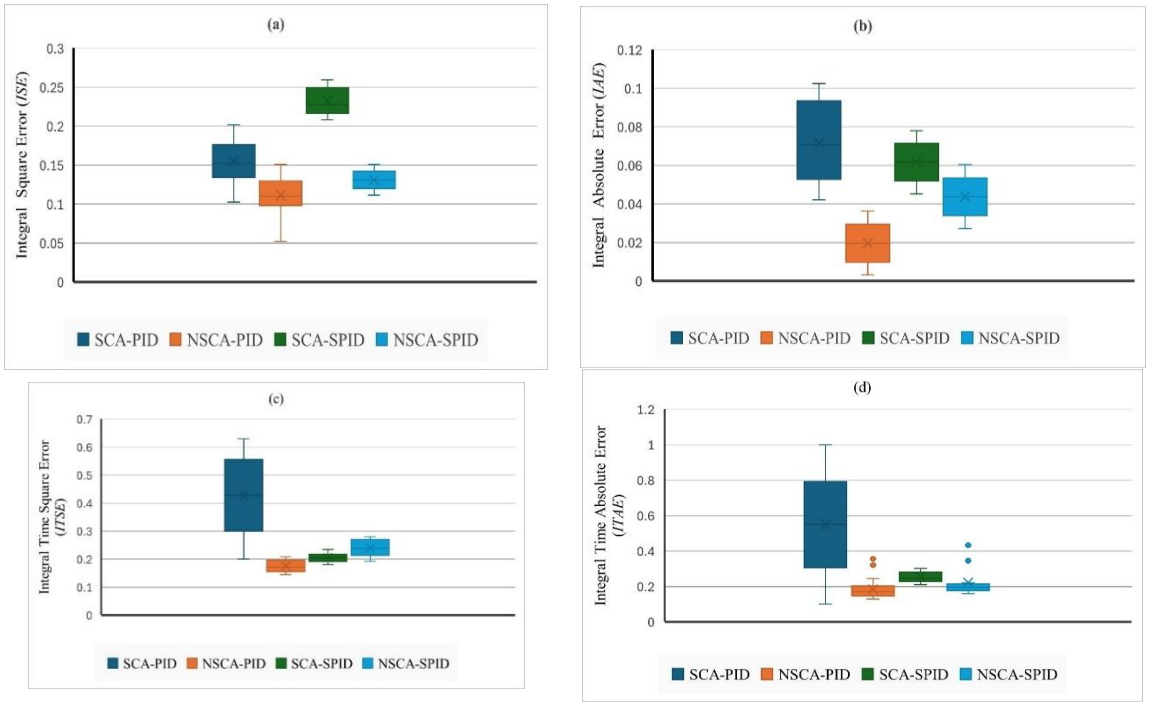

Fig. 11. Box plot of the performance indices generated by several controllers for (a) *ISE*, (b) *IAE*, (c) *ITSE*, and (d) *ITAE*

5.2. Trajectory Tracking Analysis

The following section considers the simulation of trajectory tracking as an additional case study. Finding out how successfully the suggested controller uses its terminal voltage response to follow its expected naturally is the aim of this investigation. Despite the earlier work described in [3], which used the unit step as the input reference, this study monitors the combination of the ramp and step forms of the reference signal. All these issues were resolved by aligning the reference input signal in the series with several set points to assess how well the suggested controller followed the trajectory. Despite having multiple gradients, tracking such a signal is both fascinating and challenging (see Fig. 3). Additionally, PID controller values were maintained in accordance with Table 2 and Table 3. Each controller's performance was compared using the simulation duration of T_s= 10s and the performance indices given in Eqs. (14)-(17). The outcomes of the signal trajectory tracking are displayed in Fig. 8.

The observations in that figure reveal that the proposed NSCA-SPID controller performs better than other controllers in terms of trajectory tracking response.

The numerical results obtained through ISE, IAE, ITSE, and ITAE performance indices listed in Table 6 were thoroughly validated with the results mentioned above. They have defined these performance indices according to which, smaller values indicate higher similarity between the controller response signal and the given reference signal. The values of ISE and IAE according to Table 6, demonstrate that the proposed controller represents the minimum value among other controllers. In particular, the values of the proposed NSCA-SPID controller are substantially lower than those of the others. Comparative values of ISE: The ISE value of NSCA-SPID is 0.0018 which is the smallest among other tests, showing that it is superior. The values produced by other algorithms such as SCA-PID (0.0723), GWO-PID (0.0582), and VSA-PID (0.0967) are very much higher than those.

To further evaluate each controller's effectiveness in comparisons, a trajectory tracking simulation was then run with measurement noise $e(t)$ present. The white noise $e(t)$ utilized in this case has a mean of 0 and a variance of 0.01 respectively. Additionally, the test's comparable block diagram is shown in Fig. 12. As demonstrated by the numerical results in Table 7, the proposed NSCA-SPID controller has consistently generated the lowest values in each of the four performance indices when compared to other conventional PID-based controllers. Furthermore, the system responses with noise of the proposed NSCA-SPID controller are contrasted with those of conventional PID controller-based techniques in Fig. 13.

Table 6. Comparison of several controllers' performances

Algorithms	*ISE*	*IAE*	*ITSE*	*ITAE*
hVSAGWO-PID [27]	0.0560	0.5456	0.1862	1.8760
VSA-PID [26]	0.0967	0.7207	0.2549	2.1771
GWO-PID [4]	0.0582	0.5706	0.1824	1.9151
SCA-PID [25]	0.0723	0.6052	0.2375	2.0657
Proposed NSCA-SPID	0.0018	0.1151	0.0086	0.5643

Table 7. Comparison of tracking performance in the presence of noise

Algorithms	*ISE*	*IAE*	*ITSE*	*ITAE*
hVSAGWO-PID [27]	0.1556	0.9975	0.6843	4.6451
VSA-PID [26]	0.1965	1.1172	0.7534	4.8460
GWO-PID [4]	0.1581	1.0054	0.6416	4.6363
SCA-PID [25]	0.1726	1.0510	0.7381	4.8029
Proposed NSCA-SPID	0.0646	0.5319	0.3223	2.6633

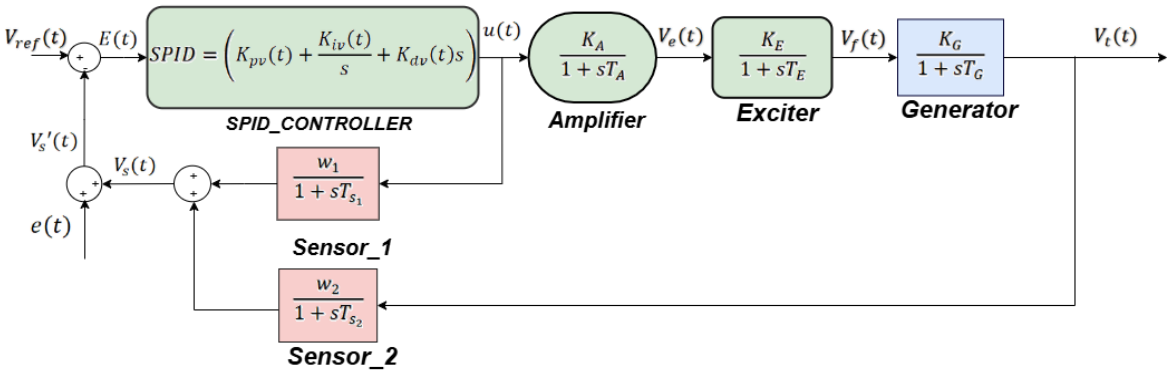

Fig. 12. AVR control system in the presence of measurement noise

First, the NSCA-SPID's *IAE* value was 0.1151, which was significantly lower than those of the other approaches, such as SCA-PID 0.6052 or VSA-PID 0.7207. Additionally, the NSCA-SPID methodology is the only one that yielded a value below 1.0 (0.5643) using the *ITAE* performance

index findings. According to this reading, the NSCA-SPID is considerably better than other methods. Additionally, NSCA-SPID consistently maintained the highest performance index score of 0.0086 out of all the approaches, and the *ITSE* value obtained using NSCA-SPID was more than five or ten times superior to that obtained using other methods. This demonstrates once more how NSCA, which has been refined by the NSCA algorithm, has a higher control efficacy than other hVSAGWO, VSA, GWO, SCA, and NSCA-based PID control methods now in application.

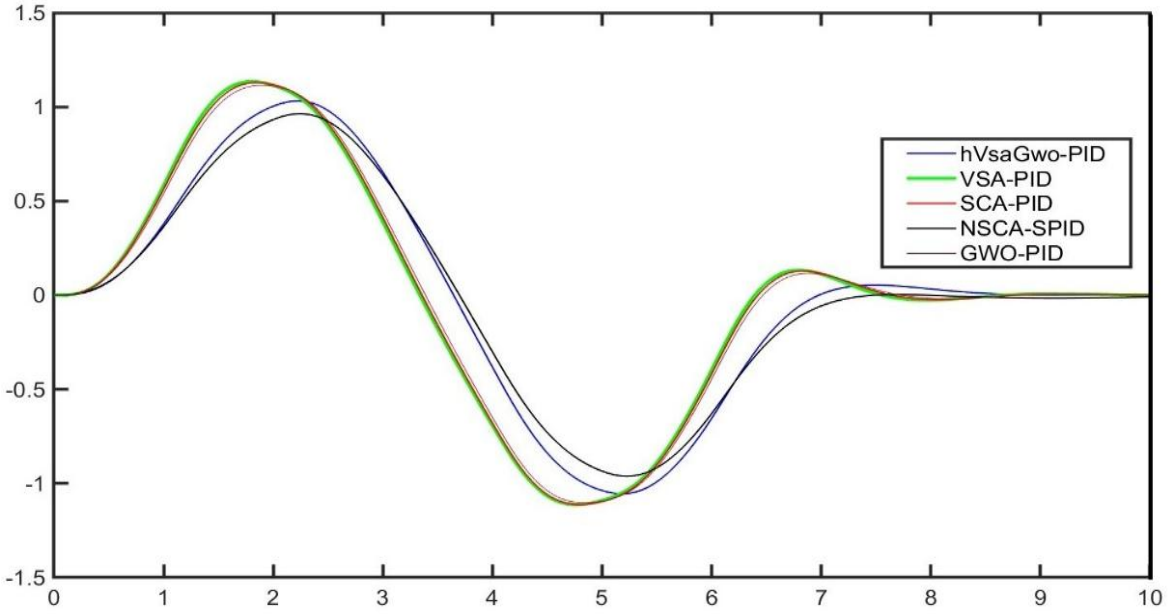

Fig. 13. System response with noise

6. Conclusion

Throughout the present research, two significant contributions resulted from the development of a proposed NSCA-SPID controller to address issues in the AVR control system. The initial contribution was integrating the recently suggested NSCA optimizer as a controller tuner, which ensured that the AVR system's parameters were optimized. In the second contribution, the amplifier feedback dynamic weighted (AFDW) 1-dof approach was introduced, which improved the system's responsiveness and robustness by dynamically adjusting the feedback weight. To further enhance the system's voltage response, the SPID controller was added to the AVR system for the first time. This control method combines the flexibility of the sigmoid-based variable structure PID, the efficacy of the NSCA optimization method, and the adaptability of the AFDW system. The NSCA-SPID outperformed conventional PID controllers, achieving the lowest ISE, IAE, ITSE, and ITAE values across a range of operating situations, according to simulation data. Additionally, the transient response analysis showed enhanced voltage control with significant reductions in overshoot and settling time while preserving an exceptional FOD value. Additionally, the efficacy of the NSCA-SPID controller for AVR system applications was validated statistically using box plots and Wilcoxon's signed-rank test.

All things considered, the results obtained demonstrate that the NSCA-SPID control system provides outstanding stability, viability, and adaptability in a variety of control scenarios. Notably, the controller is appropriate for fast-response systems such as electric vehicle induction motor drives, gantry crane systems that track trajectory, and twin-rotor MIMO systems that need maneuvering control because of its capacity to dynamically adjust to changing error conditions. In future research, the sigmoid-based PID will be replaced by a piecewise variable PID structure. Therefore, by developing a more generalized nonlinear PID controller with more control precision, it would enhance the performance of the NSCA-SPID controller.

Author Contribution: All authors contributed equally to the main contributor to this paper. All authors read and approved the final paper.

Acknowledgement: We extend our deepest gratitude to the International Islamic University Malaysia and University Malaysia Pahang for their substantial financial and resource support through the IIUM-UMP Sustainable Research Collaboration Grant 2022 (RDU223216).

Conflicts of Interest: The authors declare no conflict of interest.

References

[1] S. Chatterjee and V. Mukherjee, "PID controller for automatic voltage regulator using teaching–learning based optimization technique," *International Journal of Electrical Power & Energy Systems*, vol. 77, pp. 418-429, 2016, https://doi.org/10.1016/j.ijepes.2015.11.010.

[2] H. Gozde, "Robust 2DOF state-feedback PI-controller based on meta-heuristic optimization for automatic voltage regulation system," *ISA Transactions*, vol. 98, pp. 26-36, 2020, https://doi.org/10.1016/j.isatra.2019.08.056.

[3] S. M. A. Altbawi, A. S. B. Mokhtar, T. A. Jumani, I. Khan, N. N. Hamadneh, and A. Khan, "Optimal design of Fractional order PID controller based Automatic voltage regulator system using gradient-based optimization-algorithm," *Journal of King Saud University - Engineering Sciences*, vol. 36, no. 1, pp. 32-44, 2024, https://doi.org/10.1016/j.jksues.2021.07.009.

[4] M. H. Suid, M. A. Ahmad, S. Ahmad, M. F. M. Jusof and Z. M. Tumari, "AVR System Improvement: Fast and Optimal Tuning PID Control Using Safe Experimentation Dynamics Algorithm," *2024 International Conference on System Science and Engineering (ICSSE)*, pp. 1-5, 2024, https://doi.org/10.1109/ICSSE61472.2024.10608891.

[5] E. W. Suseno and A. Ma'arif, "Tuning of PID controller parameters with genetic algorithm method on DC motor," *International Journal of Robotics and Control Systems*, vol. 1, no. 1, pp. 41-53, 2021, https://doi.org/10.31763/ijrcs.v1i1.249.

[6] M. Faisal Farhan, N. S. Abdul Shukor, M. Ashraf Ahmad, M. Helmi Suid, M. Riduwan Ghazali, and M. F. Mat Jusof, "A simplify fuzzy logic controller design based safe experimentation dynamics for pantograph-catenary system," *Indonesian Journal of Electrical Engineering and Computer Science (IJEECS)*, vol. 14, no. 2, pp. 903-911, 2019, http://doi.org/10.11591/ijeecs.v14.i2.pp903-911.

[7] M. Nasir, M. Saloumi, and A. B. Nassif, "Review of various metaheuristics techniques for tuning parameters of PID/FOPID controllers," *ITM Web of Conferences*, vol. 43, p. 01002, 2022, https://doi.org/10.1051/itmconf/20224301002.

[8] I. A. Khan *et al*., "Load Frequency Control Using Golden Eagle Optimization for Multi-Area Power System Connected Through AC/HVDC Transmission and Supported With Hybrid Energy Storage Devices," *IEEE Access*, vol. 11, pp. 44672-44695, 2023, https://doi.org/10.1109/ACCESS.2023.3272836.

[9] D. Izci, R.M. Rizk-Allah, V. Snášel, S. Ekinci, F.A. Hashim, L. Abualigah, "A novel control scheme for automatic voltage regulator using novel modified artificial rabbits optimizer," *e-Prime - Advances in Electrical Engineering, Electronics and Energy*, vol. 6, p. 100325, 2023, https://doi.org/10.1016/j.prime.2023.100325.

[10] M. Micev, M. Ćalasan, Z. M. Ali, H. M. Hasanien, and S. H. A. Aleem, "Optimal design of automatic voltage regulation controller using hybrid simulated annealing-Manta ray foraging optimization algorithm," *Ain Shams Engineering Journal*, vol. 12, no. 1, pp. 641-657, 2021, https://doi.org/10.1016/j.asej.2020.07.010.

[11] X. Zhou, D. Li, L. Zhang, and Q. Duan, "Application of an adaptive PID controller enhanced by a differential evolution algorithm for precise control of dissolved oxygen in recirculating aquaculture systems," *Biosystems Engineering*, vol. 208, pp. 186-198, 2021, https://doi.org/10.1016/j.biosystemseng.2021.05.019.

[12] M. P. E. Rajamani, R. Rajesh, and M. W. Iruthayarajan, "A PID control scheme with enhanced non-dominated sorting genetic algorithm applied to a non-inverting buck-boost converter," *Sādhanā*, vol. 47, no. 4, p. 222, 2022, https://doi.org/10.1007/s12046-022-02012-z.

[13] A. Setiawan and P. Mudjirahardjo, "Automatic Voltage Regulator (AVR) Optimization Based on PID Using the Hybrid Grey Wolf Optimization-Genetic Algorithm (HGWGA) Method," *International Journal of Computer Applications Technology and Research*, vol. 10, no. 06, pp. 136-141, 2021, https://www.academia.edu/download/81391040/ijcatr10061002.pdf.

[14] W. BinSaeedan and S. Alramlawi, "CS-BPSO: Hybrid feature selection based on chi-square and binary PSO algorithm for Arabic email authorship analysis," *Knowledge-Based Systems*, vol. 227, p. 107224, 2021, https://doi.org/10.1016/j.knosys.2021.107224.

[15] A. Sikander, P. Thakur, R. C. Bansal, and S. Rajasekar, "A novel technique to design cuckoo search based FOPID controller for AVR in power systems," *Computers & Electrical Engineering*, vol. 70, pp. 261-274, 2018, https://doi.org/10.1016/j.compeleceng.2017.07.005.

[16] L. Kong, J.-S. Pan, and V. Snášel, "A Review of Non-dominating Sorting Algorithms," *Business Intelligence and Information Technology*, pp. 173-183, 2024, https://doi.org/10.1007/978-981-97-3980-6_15.

[17] S. B. Joseph, E. G. Dada, A. Abidemi, D. O. Oyewola, and B. M. Khammas, "Metaheuristic algorithms for PID controller parameters tuning: Review, approaches and open problems," *Heliyon*, vol. 8, no. 5, p. e09399, 2022, https://doi.org/10.1016/j.heliyon.2022.e09399.

[18] E. Kaya, B. Gorkemli, B. Akay, and D. Karaboga, "A review on the studies employing artificial bee colony algorithm to solve combinatorial optimization problems," *Engineering Applications of Artificial Intelligence*, vol. 115, p. 105311, 2022, https://doi.org/10.1016/j.engappai.2022.105311.

[19] H. Zhu, L. Li, Y. Zhao, Y. Guo, and Y. Yang, "CAS algorithm-based optimum design of PID controller in AVR system," *Chaos, Solitons & Fractals*, vol. 42, no. 2, pp. 792-800, 2009, https://doi.org/10.1016/j.chaos.2009.02.006.

[20] L. Abualigah, M. Shehab, M. Alshinwan, S. Mirjalili, and M. A. Elaziz, "Ant Lion Optimizer: A Comprehensive Survey of Its Variants and Applications," *Archives of Computational Methods in Engineering*, vol. 28, no. 3, pp. 1397-1416, 2021, https://doi.org/10.1007/s11831-020-09420-6.

[21] U. Güvenç, A. Işik, T. Yiğit, and İ. Akkaya, "Performance analysis of biogeography-based optimization for automatic voltage regulator system," *Turkish Journal of Electrical Engineering and Computer Sciences*, vol. 24, no. 3, pp. 1150-1162, 2016, https://doi.org/10.3906/elk-1311-111.

[22] A. Mishra and L. Goel, "Metaheuristic Algorithms in Smart Farming: An Analytical Survey," *IETE Technical Review*, vol. 41, no. 1, pp. 46-65, 2024, https://doi.org/10.1080/02564602.2023.2219226.

[23] A. Hashemi, M. B. Dowlatshahi, and H. Nezamabadi-Pour, "Gravitational Search Algorithm: Theory, Literature Review, and Applications," *Handbook of AI-based Metaheuristics*, 2021, https://doi.org/10.1201/9781003162841-7.

[24] R. Lozi, "Survey of recent applications of the chaotic lozi map," *Algorithms*, vol. 16, no. 10, p. 491, 2023, https://doi.org/10.3390/a16100491.

[25] A. B. Gabis, Y. Meraihi, S. Mirjalili, and A. Ramdane-Cherif, "A comprehensive survey of sine cosine algorithm: variants and applications," *Artificial Intelligence Review*, vol. 54, no. 7, pp. 5469-5540, 2021, https://doi.org/10.1007/s10462-021-10026-y.

[26] M. H. Suid and M. A. Ahmad, "Optimal tuning of sigmoid PID controller using Nonlinear Sine Cosine Algorithm for the Automatic Voltage Regulator system," *ISA Transactions*, vol. 128, pp. 265-286, 2022, https://doi.org/10.1016/j.isatra.2021.11.037.

[27] M. Saka, "Novel hVsaGwo algorithm for non-linear dynamic weighted state feedback with 1DOF-PIDbased controller," *Engineering Science and Technology, an International Journal*, vol. 59, p. 101857, 2024, https://doi.org/10.1016/j.jestch.2024.101857.

[28] F. Yang *et al*., "Adaptive disturbance compensation based finite time sliding mode frequency control considering AVR loop for low-inertia power system," *Electrical Engineering*, vol. 107, no. 4, pp. 4819-4835, 2025, https://doi.org/10.1007/s00202-024-02796-9.

[29] Y. Sun, "Analysis of the performance of PID-based new-generation metaheuristic algorithms for automatic voltage regulation system," *Proceedings of the 2023 7th International Conference on Computer Science and Artificial Intelligence*, pp. 449-454, 2023, https://doi.org/10.1145/3638584.3638622.

[30] S. M. A. Altbawi, A. S. B. Mokhtar, T. A. Jumani, I. Khan, N. N. Hamadneh, A. Khan, "Optimal design of fractional order PID controller based automatic voltage regulator system using gradient-based optimization algorithm," *Journal of King Saud University - Engineering Sciences*, vol. 36, no.1, pp. 32-44, 2024, https://doi.org/10.1016/j.jksues.2021.07.009.

[31] A. Ali, G. Biru, and B. Banteyirga, "Fuzzy logic-based AGC and AVR for four-area interconnected hydro power system," *Electric Power Systems Research*, vol. 224, p. 109494, 2023, https://doi.org/10.1016/j.epsr.2023.109494.

[32] M. Huba, P. Bistak, and D. Vrancic, "Parametrization and optimal tuning of constrained series PIDA controller for IPDT models," *Mathematics*, vol. 11, no. 20, p. 4229, 2023, https://doi.org/10.3390/math11204229.

[33] N. H. A. R. Ramesh, M. R. Ghazali, and M. A. Ahmad, "Sigmoid PID based adaptive safe experimentation dynamics algorithm of portable duodopa pump for Parkinson's disease patients," *Bulletin of Electrical Engineering and Informatics*, vol. 10, no. 2, pp. 632-639, 2021, https://doi.org/10.11591/eei.v10i2.2542.

[34] A. H. Mary, A. H. Miry, and M. H. Miry, "An Optimal Robust State Feedback Controller for the AVR System-Based Harris Hawks Optimization Algorithm," *Electric Power Components and Systems*, pp. 1684-1694, 2021, https://doi.org/10.1080/15325008.2021.1908456.

[35] T. George and V. Ganesan, "Optimal tuning of PID controller in time delay system: a review on various optimization techniques," *Chemical Product and Process Modeling*, vol. 17, no. 1, pp. 1–28, 2022, https://doi.org/10.1515/cppm-2020-2001.

[36] B. Ozgenc, M. S. Ayas, and I. H. Altas, "Performance improvement of an AVR system by symbiotic organism search algorithm-based PID-F controller," *Neural Computing and Applications*, vol. 34, no. 10, pp. 7899-7908, 2022, https://doi.org/10.1007/s00521-022-06892-4.

[37] E. S. Rahayu, A. Ma'arif, and A. Cakan, "Particle swarm optimization (PSO) tuning of PID control on DC motor," *International Journal of Robotics and Control Systems*, vol. 2, no. 2, pp. 435-447, 2022, https://doi.org/10.31763/ijrcs.v2i2.476.

[38] J. Zhang, T. Zhang, G. Zhang, and M. Kong, "Parameter optimization of PID controller based on an enhanced whale optimization algorithm for AVR system," *Operational Research*, vol. 23, no. 3, p. 44, 2023, https://doi.org/10.1007/s12351-023-00787-5.

[39] S. B. Joseph, E. G. Dada, A. Abidemi, D. O. Oyewola, and B. M. Khammas, "Metaheuristic algorithms for PID controller parameters tuning: Review, approaches and open problems," *Heliyon*, vol. 8, no. 5, p. e09399, 2022, 2025, https://doi.org/10.1016/j.heliyon.2022.e09399.

[40] A. Bouaddi, R. Rabeh, and M. Ferfra, "Optimal control of automatic voltage regulator system using hybrid PSO-GWO algorithm-based PID controller," *Bulletin of Electrical Engineering and Informatics*, vol. 13, no. 5, pp. 3070-3080, 2024, https://doi.org/10.11591/eei.v13i5.8186.

[41] S. Veinović, D. Stojić, and D. Joksimović, "Optimized four-parameter PID controller for AVR systems with respect to robustness," *International Journal of Electrical Power & Energy Systems*, vol. 135, p. 107529, 2022, https://doi.org/10.1016/j.ijepes.2021.107529.

[42] A. Sivanandhan, G. Thriveni, "Optimal design of controller for automatic voltage regulator performance enhancement: a survey," *Electrical Engineering*, vol. 106, pp. 3705-3720, 2025, https://doi.org/10.1007/s00202-023-02196-5.

[43] A. K. Sahin, B. Cavdar, and M. S. Ayas, "An adaptive fractional controller design for automatic voltage regulator system: sigmoid-based fractional-order PID controller," *Neural Computing and Applications*, vol. 36, no. 23, pp. 14409-14431, 2024, https://doi.org/10.1007/s00521-024-09816-6.

[44] J. Bhookya and R. K. Jatoth, "Optimal FOPID/PID controller parameters tuning for the AVR system based on sine–cosine-algorithm," *Evolutionary Intelligence*, vol. 12, pp. 725-733, 2019, https://doi.org/10.1007/s12065-019-00290-x.

[45] A. B. Gabis, Y. Meraihi, S. Mirjalili, and A. Ramdane-Cherif, "A comprehensive survey of sine cosine algorithm: variants and applications," *Artificial Intelligence Review*, vol. 54, no. 7, pp. 5469-5540, 2021, https://doi.org/10.1007/s10462-021-10026-y.

[46] B. Hekimoğlu, "Sine-cosine algorithm-based optimization for automatic voltage regulator system," *Transactions of the Institute of Measurement and Control*, vol. 41, no. 6, pp. 1761-1771, 2019, https://doi.org/10.1177/0142331218811453.

[47] R. Roque Yujra and F. J. Triveño Vargas, "Performance and Robustness of the Response of an AVR with Optimized PID Using the Sine Cosine Algorithm (SCA)," *Acta Nova*, vol. 10, no. 3, pp. 303-317, 2022, https://www.researchgate.net/publication/373301533_Performance_and_Robustness_of_the_Response_of_an_AVR_with_Optimized_PID_Using_the_Sine_Cosine_Algorithm_SCA.

[48] A. Yakout, H. Kotb and W. Sabry, "Power Oscillation Damping using Sine Cosine Algorithm based Tilt-Derivative Tilt-Integral Automatic Voltage Regulator," *2022 23rd International Middle East Power Systems Conference (MEPCON)*, pp. 1-5, 2022, https://doi.org/10.1109/MEPCON55441.2022.10021745.

[49] A. B. Gabis, Y. Meraihi, S. Mirjalili, and A. Ramdane-Cherif, "A comprehensive survey of sine cosine algorithm: variants and applications," *Artificial Intelligence Review*, vol. 54, no. 7, pp. 5469-5540, 2021, https://doi.org/10.1007/s10462-021-10026-y.

[50] M. Y. Silaa, O. Barambones, M. Derbeli, C. Napole, and A. Bencherif, "Fractional order PID design for a proton exchange membrane fuel cell system using an extended grey wolf optimizer," *Processes*, vol. 10, no. 3, p. 450, 2022, https://doi.org/10.3390/pr10030450.

[51] T. Peng, Y. Wu, L. Huang, B. He, and S. Wei, "Acupuncture for chronic pelvic pain in patients with SPID: a protocol for systematic review and meta-analysis," *Medicine*, vol. 100, no. 4, p. e23916, 2021, https://doi.org/10.1097/MD.0000000000023916.

[52] B. Verma and P. K. Padhy, "Tuning of PID controller using sigmoidal weighted error function," *2017 Innovations in Power and Advanced Computing Technologies (i-PACT)*, pp. 1-5, 2017, https://doi.org/10.1109/IPACT.2017.8245083.

[53] S. Ekinci, B. Hekimoğlu, A. Demirören and E. Eker, "Speed Control of DC Motor Using Improved Sine Cosine Algorithm Based PID Controller," *2019 3rd International Symposium on Multidisciplinary Studies and Innovative Technologies (ISMSIT)*, pp. 1-7, 2019, https://doi.org/10.1109/ISMSIT.2019.8932907.

[54] N. Merayo *et al*., "PID controller based on a self-adaptive neural network to ensure qos bandwidth requirements in passive optical networks," *Journal of Optical Communications and Networking*, vol. 9, no. 5, pp. 433-445, 2017, https://doi.org/10.1364/JOCN.9.000433.

[55] M. H. Suid, M. A. Ahmad, A. N. K. Nasir, M. R. Ghazali, and J. J. Jui, "Continuous-time Hammerstein model identification utilizing hybridization of Augmented Sine Cosine Algorithm and Game-Theoretic approach," *Results in Engineering*, vol. 23, p. 102506, 2024, https://doi.org/10.1016/j.rineng.2024.102506.

[56] J. J. Jui, M. A. Ahmad, "A hybrid metaheuristic algorithm for identification of continuous-time Hammerstein systems," *Applied Mathematical Modelling*, vol. 95, pp. 339-360, 2021, https://doi.org/10.1016/j.apm.2021.01.023.

[57] M. R. Ghazali, M. A. Ahmad and R. M. T. R. Ismail, "Data-Driven PID Control for DC/DC Buck-Boost Converter-Inverter-DC Motor based on Safe Experimentation Dynamics," *2018 IEEE Conference on Systems, Process and Control (ICSPC)*, pp. 89-93, 2018, https://doi.org/10.1109/SPC.2018.8704161.

[58] E. -S. M. El-Kenawy *et al*., "Advanced Ensemble Model for Solar Radiation Forecasting Using Sine Cosine Algorithm and Newton's Laws," *IEEE Access*, vol. 9, pp. 115750-115765, 2021, https://doi.org/10.1109/ACCESS.2021.3106233.

[59] Q. Jin and M. Cui, "Chaotic salp swarm algorithm: Application to parameter identification for MIMO Hammerstein model under heavy tail noise," *2020 12th International Conference on Intelligent Human-Machine Systems and Cybernetics (IHMSC)*, pp. 264-268, 2020, https://doi.org/10.1109/IHMSC49165.2020.00066.

[60] R. Lotfi, R. M. Shafiei, M. G. Komeleh, F. G. Pasha, M. Ferasat, "Vaccine supply chain network design by considering viability, robustness and risk," *Journal of Engineering Research*, vol. 13, no. 1, pp. 23-38, 2024, https://doi.org/10.1016/j.jer.2023.10.007.